JOURNAL OF GEOPHYSICAL RESEARCH, VOL. 95, NO. D3, PAGES 2195–2205, FEBRUARY 28, 1990

Sampling Errors for Satellite-Derived Tropical Rainfall: Monte Carlo Study Using a Space-Time Stochastic Model

THOMAS L. BELL

Laboratory for Atmospheres, Goddard Space Flight Center, Greenbelt, Maryland

A. ABDULLAH AND RUSSELL L. MARTIN

Applied Research Corporation, Landover, Maryland

GERALD R. NORTH

College of Geosciences, Texas A&M University, College Station

Estimates of monthly average rainfall based on satellite observations from a low Earth orbit will differ from the true monthly average because the satellite observes a given area only intermittently. This sampling error inherent in satellite monitoring of rainfall would occur even if the satellite instruments could measure rainfall perfectly. We estimate the size of this error for a satellite system being studied at NASA, the Tropical Rainfall Measuring Mission (TRMM). We first examine in detail the statistical description of rainfall on scales from 1 to 10^3 km, based on rainfall data from the Global Atmospheric Research Project Atlantic Tropical Experiment (GATE). A TRMM-like satellite is flown over a two-dimensional time-evolving simulation of rainfall using a stochastic model with statistics tuned to agree with GATE statistics. The distribution of sampling errors found from many months of simulated observations is found to be nearly normal, even though the distribution of area-averaged rainfall is far from normal. For a range of orbits likely to be employed in TRMM, sampling error is found to be less than 10% of the mean for rainfall averaged over a 500×500 km^2 area.

1. INTRODUCTION

A significant fraction of the heating of the tropical atmosphere comes from latent heat released in precipitating clouds. The formation of rain in the tropics is thus an important step in a process that transforms the energy in incoming solar radiation into kinetic energy of the atmosphere. Accurate estimates of the amount of rainfall in the tropics would substantially improve our knowledge of the workings of weather and climate, but tropical rainfall is not very well monitored, since much of the tropics is covered by ocean. Continuous coverage of these large oceanic expanses is probably only feasible from space. Present-day satellite measurements of rainfall, however, rely on relatively indirect methods and are not always easy to verify quantitatively.

A remedy for this situation, a satellite designed specifically to measure rainfall as accurately as possible from space, is presently being planned. It will be referred to as the Tropical Rainfall Measuring Mission (TRMM). *Simpson et al.* [1988] discuss in detail the need for the satellite and the kinds of instruments presently envisaged for it.

A primary goal of TRMM will be to provide accurate monthly averages of tropical rainfall within areas of the order of 500×500 km^2. There will be two sources of error in these averages, broadly speaking: the error inherent in the method used to determine rain rate at a given instant, and the "sampling" error associated with the satellite's only being able to observe a given area intermittently.

Paper number 89JD01655.
0148-0227/90/89JD-01655$05.00

The impact of the first source of error, retrieval error, may in principle be considerably reduced by taking monthly averages of the data over large enough areas, provided retrieval algorithms can be developed that generate unbiased estimates of rainfall (no small task!). The radar system included in the TRMM instrument package, combined with extensive ground-based verification, will help considerably in calibrating satellite retrievals. A rough estimate of retrieval error is given in the appendix.

The second source of error, arising from intermittent observation by the satellite, is determined by the orbit of the satellite and the size of the swath scanned by the satellite as it passes over, and by the statistical characteristics of the observed rainfall. It is the dominant contribution to the error in monthly averages if systematic error in the retrieval algorithms is small. It is with this kind of error that we shall be chiefly concerned here.

The size of this error depends on how well sampled the area is during a month. We shall describe here a baseline calculation of sampling error assuming that information is available only from the TRMM satellite itself. Clearly the error can be reduced by adding information from other satellites or ground stations, and this will almost certainly be attempted. One of the potential benefits TRMM offers is the "calibration" of infrared and microwave instruments on other satellites so that their data can be converted into rainfall estimates where TRMM data are unavailable.

Although we shall focus on the particular observational configuration offered by TRMM, the methods we develop here are obviously applicable to studies of sampling errors for other satellite systems monitoring other geophysical quantities.

As a measure of error, we shall use the root mean square (rms) difference between the actual rain rate averaged over a month and the mean of the satellite observations during that month. The true monthly averaged rain rate is

$$R = \frac{1}{T}\int_0^T dt\,\frac{1}{A}\int_A d^2\mathbf{x}\; r(\mathbf{x}, t) \tag{1}$$

where $r(\mathbf{x}, t)$ is the rain rate at location $\mathbf{x}$, t is the time since the beginning of the month, and T and A are the period (1 month) and area averaged over.

The satellite observes the area A sporadically, at times t_i during the month, and does not always observe the entire area A but only some subarea A_i,

$$A_i = f_i A \tag{2}$$

where f_i is the fraction of the area observed. If we let

$$r_i = \frac{1}{A_i}\int_{A_i} d^2\mathbf{x}\; r(\mathbf{x}, t_i) \tag{3}$$

be the subarea-averaged rainfall, then a satellite-based estimate of the true rainfall R can be written as

$$\hat{R} = \sum_{i=1}^{M} w_i r_i \tag{4}$$

where M is the number of overflights of the area during the period T, and w_i are factors that might in principle be adjusted to improve the estimate $\hat{R}$ as much as possible, depending on the spatial and temporal correlations of the rainfall. Here we shall simply assume that each observation at each point in the area is to be given equal weight, so that the factors w_i are just proportional to A_i,

$$w_i = f_i \Big/ \sum_{i=1}^{M} f_i \tag{5}$$

They have been normalized to given an unbiased estimate of R.

The rms error E can then be written in terms of these definitions as

$$E^2 \equiv \langle (\hat{R} - R)^2 \rangle \tag{6}$$

where the angle brackets indicate an average over an ensemble of possible histories of rainfall during the month. The error E represents the typical size of errors in satellite estimates of monthly averaged rain over many months of observations or over many climatologically similar areas. Implicit in using rms error is the idea that the errors $\hat{R} - R$ might be approximately normally distributed with standard deviation E. We shall find that this is the case in our simulations, even though the instantaneous area-averaged rainfall is far from being normally distributed.

The rms error E in (6) is in principle completely determined by the covariance statistics of point rainfall. It is a difficult and subtle task, however, to extrapolate the statistics obtained from rain gauges to the area and time averages needed in (6) because the spatial and temporal variability of rainfall is so extreme. The areal coverage provided by radar is more nearly comparable to the averaging areas to be used for TRMM, but well-calibrated data from the tropical oceanic regions are not easy to find. In the study presented here we have in fact limited ourselves to radar data collected in the Global Atmospheric Research Program Atlantic Tropical Experiment (GATE) during the summer of 1974. This paucity of tropical radar data should be ameliorated in the near future as ground-based experiments associated with TRMM get under way.

An early attempt at obtaining E was made by *Laughlin* [1981], who estimated it for a satellite that visits the area at equal intervals Δt and views the entire area each time. He was able to write E^2 in terms of the variance of the area-averaged rain rate σ_A^2, and of the correlation time of the area-averaged rain rate, τ_A, as

$$E^2 = \sigma_A^2 f(\Delta t, \tau_A, T) \tag{7}$$

His derivation is reviewed by *Shin and North* [1988], who have improved on his method by taking into account the actual visit times of the satellite and fractional coverage of the visits. They make the approximations that the statistics of area-averaged rainfall not depend on the size of the area averaged over, and that repeated visits occurring less than a few hours apart be counted as a single observation. The first approximation tends to lead to underestimates of the error, since rainfall in smaller areas has greater variance and shorter time scales than rainfall averaged over larger areas. The second approximation, however, tends to overestimate the error.

Our approach here will be to simulate the rainfall over an area with a statistical model, and to "fly" a satellite in a TRMM-like orbit over the simulated rainfall, computing the rms error (6) from multiple trials each a month long. The rainfall model is adjusted to have spatial and temporal variability with covariance statistics matching those observed in GATE. Some choices must be made in extrapolating the GATE results to spatial and temporal scales larger than those of GATE, and will be discussed here. These choices affect the size of E.

The advantages of the Monte Carlo approach are that it offers a covenient vehicle for including in the calculation of E the effects of the dependence of rainfall statistics on the fraction of the area observed by the satellite during a given pass; and it gives some insight into the probability distribution of errors. The disadvantages are that it gives results whose accuracy depends on the number of months in the simulation and, as always, the results depend on the ability of the model to capture the relevant statistics of real rain.

We find that, for the cases we have studied, *Laughlin*'s [1981] original method gives a fair account of the error, at least for areas near the equator, where the satellite observations are roughly equally spaced in time and his calculations are applicable, and *Shin and North*'s [1988] extension seems to underestimate E by only 10% or 20% (of E).

In section 2 we review the sampling characteristics of the satellite. Section 3 contains a brief description of the rainfall model. Section 4 describes the model parameter choices made in extrapolating rainfall statistics to the climatological scales of interest. Section 5 describes the Monte Carlo experiments. Sampling error estimates are given in section 6, and their probability distribution is explored in section 7. Further discussion and conclusions are offered in section 8. The impact of retrieval error is evaluated in the appendix.

2. SAMPLING CHARACTERISTICS OF THE SATELLITE

The sampling error E defined in (6) depends on the sequence of satellite observing times t_i and observed subareas A_i, since this sequence determines the accuracy of the estimate $\hat{R}$ in (4). In generating sequences typical of the TRMM satellite, it was assumed that the orbit of the satellite would be nearly circular and that the deviations from a strict Keplerian orbit would be mostly accounted for by including the effects of the Earth's quadrupole gravitational field, which are to modify the orbital period slightly and to cause the orbital plane to precess. The parameters of the orbits are calculated following the procedures described by *Brooks* [1977]. A summary of these procedures is given by *Shin and North* [1988].

The viewing characteristics of the satellite are assumed to be similar to those of the electrically scanning microwave radiometer (ESMR) flown on the Nimbus V satellite. The ESMR measured the intensity of microwave radiation at 19.35 GHz in 78 fields of view (FOVs) during each scan of the instrument. The instrument scanned perpendicularly to the direction of the satellite motion, from 50° to the left of nadir to 50° to the right of nadir, requiring 4 s per scan. The beam widths of the FOVs (at −3 dB) ranged from 1.4° × 1.4° near nadir to 1.4° × 2.2° at the 50° extremes [*Wilheit*, 1972]. The FOV was defined to include all grid boxes of the rainfall model (4-km boxes) near enough to the center of the FOV that an exponential fit to the antenna response at the grid box center exceeds −7 dB (about 0.2 of the power received on the antenna axis). With this (perhaps slightly liberal) choice, the FOVs overlap substantially, and nearly complete coverage of the area within the view of the satellite is assured. It implies that in our calculations the effective size of the swath extends to about 54° on either side of nadir.

As an example of the sampling characteristics of such a satellite, we plot in Figure 1 the times during 1 month when the satellite is able to view any portion of a 500 × 500 km^2 box centered at either latitude 5° or 25°N. The satellite is in a 35° inclination orbit at 350-km altitude. The plots illustrate two features of low-inclination satellite orbits: (1) sampling times vary with the local time, so that the complete diurnal cycle may be explored during 1 month, and (2) for regions near the equator the observations are nearly equally spaced in time; at higher latitudes the observations increase in number but are bunched together in time so that a long period with no observations occurs each day.

The whole of the box is not seen each time, but only some fraction f_i. As a measure of how many times per day a given point in a box is observed, consider the average

$$\bar{f} = \lim_{T\to\infty} \frac{1}{T} \sum_{i=1}^{M} f_i \tag{8}$$

which is shown in Figure 2 as a function of latitude for the same orbit as for Figure 1. Here M is the number of observations of the box during the interval T. Figure 2 reveals that at latitude 5°N, even though there are several encounters with the box per day, only slightly more than half the box is seen on any one visit, on average. At the very highest latitudes the satellite is able to view only the southernmost (or northernmost, depending on the hemisphere) portion of the 500 × 500 km^2 box.

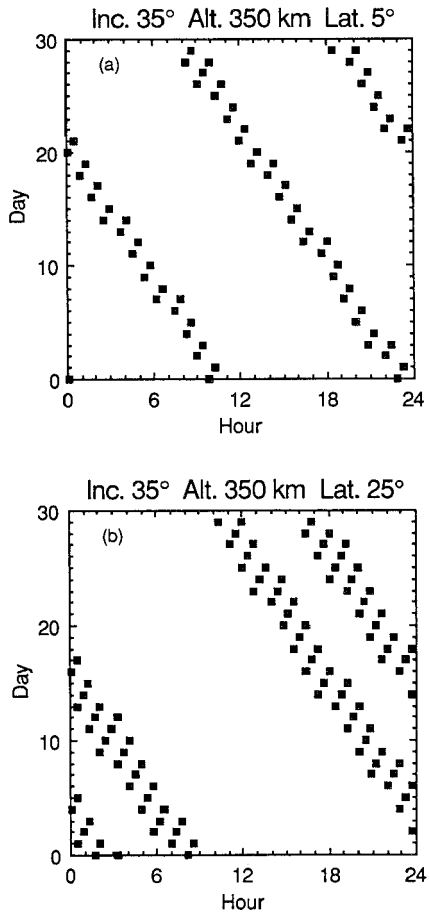

Fig. 1. Viewing times of a 500 × 500 km^2 box during 1 month for a satellite with orbital inclination 35°, altitude 350 km, and scanning 54° to the left and right of nadir. (Top) Box center at 5°N and (bottom) box center at 25°N.

3. MODEL DESCRIPTION AND STATISTICS

The model we use in our rainfall simulations is described in detail by *Bell* [1987*a*]. We summarize its features here briefly.

The model generates a field of rain rates on a grid, the value at each grid point representing the rain rate averaged over the surrounding grid square. The field evolves in time.

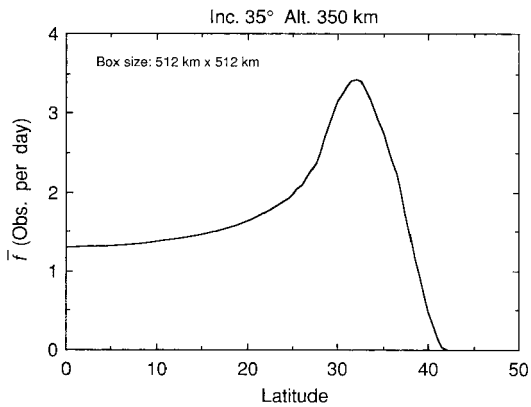

Fig. 2. Mean number of observations per day of points in a 500 × 500 km^2 box, averaged over the box, as a function of the latitude of the box center, for the satellite orbit of Figure 1. See (8).

The distribution of nonzero rain rates generated at any one grid point is lognormal in the current implementation of the model. (Properties of the lognormal distribution are reviewed by *Aitchison and Brown* [1963].) The fraction of time that it rains, and the mean and standard deviation of the logarithm of nonzero rain rates, must be supplied. These parameters determine the time-averaged statistics of rain rate at each grid point of the model. The fraction of the area with nonzero rain varies from moment to moment as the rain field evolves.

The model should generate rain rate fields with spatial and temporal covariances that agree as well as can be managed with those found in nature, since the error (6) is entirely dependent on these statistics. The model requires that these statistics be supplied, and the choices made for them will be discussed in section 4.

The model is based on the possibility of generating a correlated field of variables that are multivariate Gaussian, by the standard technique of expressing it as a sum of uncorrelated Fourier components,

$$g(\mathbf{x}) = \sum_{\mathbf{k}} a(\mathbf{k}) \exp(i\mathbf{k}^T\mathbf{x}) \tag{9}$$

where $\mathbf{x}$ labels grid points on an $N \times N$ grid,

$$\mathbf{x} = (m_1, m_2) \qquad 0 \le m_i \le N - 1 \tag{10}$$

with some specified spacing (4 km in our simulations) and m_i, $i = 1, 2$, are integers. The components of the wave vector $\mathbf{k}$ ($0 \le k_i < 2\pi$) take values that are multiples of the frequency $2\pi/N$. The product $\mathbf{k}^T\mathbf{x}$ denotes $k_1x_1 + k_2x_2$. The transformation (9) can be carried out very rapidly numerically using "fast-Fourier transform" (FFT) methods that are commonly available on mainframe computer systems.

The real and imaginary parts of the coefficients $a(\mathbf{k})$ are uncorrelated Gaussian random variables (uncorrelated except for the constraints required to generate only real $g(\mathbf{x})$). The variances of these random coefficients depend on $\mathbf{k}$ and are determined by the spatial correlations of the field $g(\mathbf{x})$ by

$$\langle a_{\mathbf{k}}^* a_{\mathbf{k}} \rangle = N^{-2} \sum_{\mathbf{x}} c_g(\mathbf{x}) \exp(-i\mathbf{k}^T\mathbf{x}) \tag{11}$$

where $c_g(\mathbf{x})$ is the correlation of g at two grid points separated by $\mathbf{x}$.

Rain rates $r(\mathbf{x})$ are obtained from the Gaussian variables $g(\mathbf{x})$ with a transformation $\mathcal{R}$,

$$r = \mathcal{R}(g) \tag{12}$$

where $\mathcal{R}$ is 0 for values of g below some threshold g_0 (chosen so that the probability of generating zero rain rate ($r = 0$) agrees with observed probabilities) and increases smoothly from 0 for values of $g > g_0$ in such a way that the rain rates generated are lognormally distributed when the variable g is normally distributed (g is assumed to have mean 0 and variance 1). A rough physical interpretation of the model might be that the field $g(\mathbf{x})$ represents a horizontal convergence field or vertical velocity field, and rain occurs where the convergence is sufficiently strong.

Since it is the spatial covariance of the rain rate $r(\mathbf{x})$ that is specified rather than the correlations of the field $g(\mathbf{x})$, the correlation $c_g(\mathbf{x})$ must be adjusted so that it generates the desired rain field covariances. This can be done and is described by *Bell* [1987*a*].

Correlations in time are introduced by generating time-dependent coefficients $a(\mathbf{k}, t)$ with a first-order autoregressive process with correlation times $\tau_{\mathbf{k}}$ that depend on wave vector $\mathbf{k}$. This is the one feature of the model that is not straightforward to tune to agree with correlations observed in rainfall data. We shall describe how these correlation times were chosen in the next section, after discussing the choices made for the other parameters in the model.

4. Parameter Values of the Model Based on GATE

We discuss here the actual parameter choices for the model. They are based on statistics obtained from radar data collected during GATE in the tropical Atlantic in the vicinity of the Intertropical Convergence Zone (ITCZ). The data were converted into gridded rainfall values on a 4-km grid by *Hudlow and Patterson* [1979]. Although the data were taken well off the coast of Africa, their statistics may be affected by easterly waves coming from the continent [e.g., *Houze and Betts*, 1981], and it is not easy to say whether they are typical of mid-ocean rainfall statistics. Nevertheless, for lack of any comparable data set in the tropical ocean environment, we shall base our model parameters on GATE statistics.

The model grid is given the same spacing as the gridded GATE data, 4 km. One could in principle use a coarser grid, with suitably altered statistics, to make the model computationally faster. The number of grid points in the simulation, N in (10), is best set at some power of 2, in order to take maximum advantage of the FFT algorithm, and so the simulations are carried out with $N = 256$. This means that the model generates 1024×1024 km^2 rain fields, which, however, must be divided into four quadrants because of the periodicity inherent in Fourier synthesis (see *Bell* [1987*a*] for further discussion). The model thus generates four rain fields, each 512×512 km^2 in size on a 4-km grid. Each 300-day simulation, with a 1-hour time step, requires 20 min on a Control Data Corp Cyber 205 computer.

4.1. *Point Statistics*

With the model resolution determined, we must next specify the parameters of the mixed lognormal distribution for rain rate at any grid point. These are taken from a study by *Kedem et al.* [1990] of the GATE data, who find that the lognormal distribution fits gridded rain rates $r > 1$ mm/h quite well. Since rain rates $r < 1$ mm/h account for only a few percent of the total rain volume in GATE, and the accuracy of these low rain rate data themselves is in any case not easy to assess, we shall assume the lognormal distribution applies to all nonzero rain rates. *Kedem et al.*[1990] fit the GATE data sampled at different spatial and temporal intervals; we use parameters from their most densely sampled study of the GATE phase I (June 28 to July 16, 1974) period. The parameters are given in Table 1. Here p is the fraction of time it rains at a grid point, and the mean μ and variance σ^2 of ln r define the lognormal distribution.

Using these parameters, we can calculate the expected mean and variance of the rain rates, at 4-km resolution, generated in our simulations:

$$\langle r \rangle = pe^{\mu + \sigma^2/2} = 0.445 \text{ mm/h} \tag{13a}$$

TABLE 1. Parameters of the Rainfall Model Used in Simulations

Parameter	Value	Comment
Grid spacing	4 km	
Simulation area	512×512 km^2	per quadrant
Grid point rain statistics	$p = 0.083$	probability of rain
	$\mu = 1.13$	mean of ln r for $r > 0$
	$\sigma^2 = 1.1$	variance of ln r for $r > 0$
Spatial correlation ($s \geq 4$ km)	$c_r(s) = \dfrac{\exp(-s/a_4)}{(a_1 s + a_2)^{a_3}}$	$a_1 = 1.193$
		$a_2 = -2.165$
		$a_3 = 0.2902$
		$a_4 = 78.11$
Temporal correlation (correlation times for a_k)	$\tau_k = 21\,(2\pi/512k)^{0.94}$	hours
	$\tau_{k=0} = 21$	hours

Note that the time scales τ_k describe the Gaussian field g, not the rain field r.

$$\text{var}\,(r) = p^2 e^{2\mu + 2\sigma^2} - \langle r \rangle^2 = 7.0\ \text{mm}^2/\text{h}^2 \qquad (13b)$$

4.2. *Spatial Correlation*

The spatial correlation of the Gaussian field $g(\mathbf{x})$ is needed (11), and to obtain that we need the spatial correlation of GATE rainfall. The largest square area that fits within the 400-km diameter GATE area is 280 km on a side, scarcely a third of the 512×512 km^2 area of our simulation. Some extrapolation to larger scales will thus be necessary. Correlations have been computed for phase I and phase II (July 24 to August 15, 1974) of GATE, assuming that the correlations are homogeneous over the GATE area and isotropic (independent of direction), so that spatial and directional averaging could be used to reduce the sampling errors in the correlations. The true correlations are probably not perfectly homogeneous or isotropic, but since we are calculating satellite sampling error averaged over an area that is not highly elongated, using statistics averaged over a large area and all directions is a good first approximation. Anisotropy and inhomogeneity effects are more serious considerations in developing statistical interpolation procedures for rainfall data.

The spatial correlations are plotted in Figure 3 as a function of separation s, as well as two analytical fits to the GATE I correlations. The fit labeled A in Figure 3 is given in Table 1 and is used in the simulations. The curve labeled B is very nearly a power law: it is fit to the correlations for $s \leq 72$ km, and is given by *Bell* [1987*a*] as

$$c_r(s) = (0.25s + 0.63682)^{-2/3} \qquad s \geq 4\ \text{km} \qquad (14)$$

A careful study of the statistical uncertainty in the correlation at $s = 80$ km indicates that the correlation at this separation is known to an accuracy of ± 0.1 (95% confidence limits). It is therefore not clear whether the two GATE phases have significantly different spatial correlations. Since both GATE phases seem to yield correlations that fall off faster than the power law fit for large s, an exponential factor with an e-folding scale of about 80 km is included in the analytical fit, as indicated in Table 1.

It was mentioned in the introduction that *Laughlin* [1981] derived the error E for the special case of uniform sampling of an area and found it was proportional to the rms area-averaged rain rate, σ_A, as shown in (7). Since σ_A governs the overall scale of E, it is instructive to compare the variance of area-averaged rain rate found in GATE with what the rainfall model will generate. The latter can be obtained analytically.

If we denote the area-averaged rain rate for the model by

$$\overline{r_A} = \frac{1}{L^2} \sum_{\mathbf{x} \in A} r(\mathbf{x}) \Delta A \qquad (15)$$

where the sum is over all grid points within the area $A = L^2$ and ΔA is the area of a grid box, $\Delta A = 16$ km^2, then we can write the variance of the area average (15) in terms of the rain correlation as

$$\sigma_A^2 = \frac{\text{var}\,(r)}{N^4} \sum_{m_1 = -N}^{N} \sum_{m_2 = -N}^{N} (N - |m_1|)(N - |m_2|) c_r(\mathbf{m}) \qquad (16)$$

where $c_r(\mathbf{m})$ is the correlation of rain rates at two grid points separated by $\mathbf{m}$, and

$$N = L/(4\ \text{km}) \qquad (17)$$

so that L^2 is the number of grid points in the area A. Equation (16) is the discrete two-dimensional analog of the equation for the variance of time averages discussed by *Leith* [1973].

Using GATE data for phase I, σ_A^2 was computed for various sizes of A (results courtesy of A. McConnell and L. S. Chiu, private communication, 1987). To reduce sampling

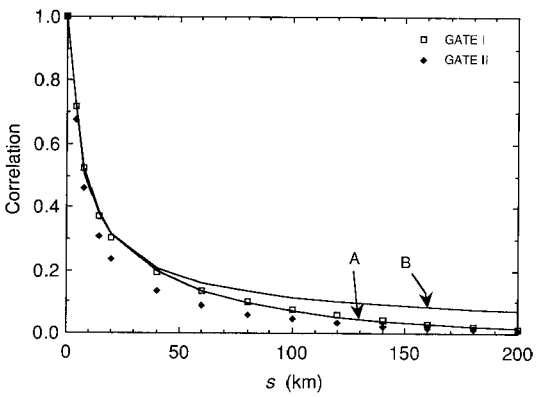

Fig. 3. Spatial correlation of gridded GATE rainfall for phases I and II as a function of separation s. Curve A shows the analytical fit employed in the simulations, given in Table 1. Curve B shows a near-power-law fit (to data for $s \leq 72$ km) given in (14).

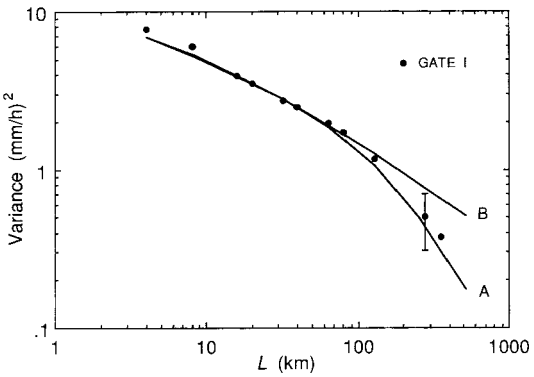

Fig. 4. Variance of area-averaged rainfall for GATE phase I as a function of the size of the area $A = L^2$. The error bar on the point at $L = 280$ km shows the 95% confidence limits assuming normal statistics and an 8-hour correlation time, and is therefore probably too small. The point for the largest area is actually for the entire 400-km-diameter GATE area, assigned an equivalent value of $L = 350$ km. Curves A and B show the predicted variances based on (16) and the two spatial correlation fits in Figure 3.

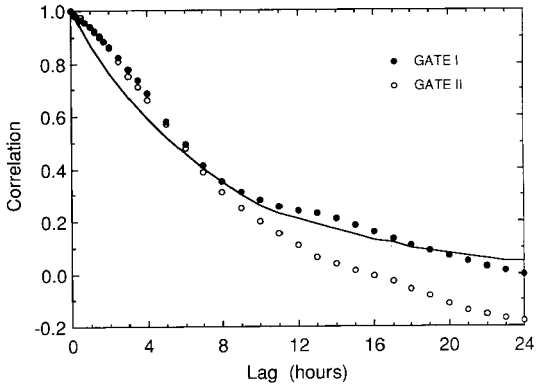

Fig. 5. Lagged correlations for model (curve) and GATE phases I and II (solid and open circles) for rainfall averaged over 280 × 280 km^2 area.

errors for a given size of A, variances obtained for areas centered on many different locations within the GATE region were averaged together. The results are shown in Figure 4. The variances shown here differ from those reported by *Laughlin* [1981] because of the average over many locations of A. Also shown in Figure 4 is the estimated uncertainty in σ_A^2 for $L = 280$ km, with the error bar indicating 95% confidence limits. This estimate is based on the assumptions that $\overline{r_A}(t)$ is normally distributed and has a correlation time of approximately 8 hours (discussed later in this section). The assumption of normality is not a very good one, as we shall see, and so this error estimate may be too small.

Superimposed on the GATE I results in Figure 4 are curves obtained using (16). The curve labeled A is based on the statistics specified in Table 1. The curve labeled B uses instead the correlation given in (14) but the same lognormal point statistics [i.e., the same var (r)]. Note that the two extrapolations to the scale of interest to us ($L = 512$ km) lead to values of σ_A differing by a factor of 1.7. This implies that if we were to use the approximate power law fit (14), we would estimate E to be perhaps 1.7 times as large as what we shall obtain. Note too that even at these scales the variance σ_A^2 is not falling off as fast as $1/A$, as would be the case if there were less spatial correlation.

4.3. *Time Correlation*

We turn next to the specification of the time correlations in the model, which are governed by the time correlations of the coefficients $a(\mathbf{k}, t)$ in (9) for $g(\mathbf{x}, t)$. (Time correlations of the model on small scales are also affected by overall advection of the rain field with a speed of 4 m/s, introduced to match typical advection speeds observed in the GATE region [*Houze and Cheng*, 1977].) It is not straightforward to relate the time correlations of the rain field $r(\mathbf{x}, t)$ to those of the field $g(\mathbf{x}, t)$ because of the effect of the intervening nonlinear transformation $\mathcal{R}$ in (12). Using Newton's method, however, we can reproduce the time correlations of the GATE data as accurately as we like within the constraints of using an autoregressive process for time evolution of the model.

Rather than examine the time correlations of Fourier amplitudes, we shall use the lagged correlations of area-averaged rain to reflect the scale dependence of correlation times. We shall define the correlation time to be the lag for which correlation drops to $1/e \approx 0.37$, rather than by fitting the lagged correlation to an exponential, as *Laughlin* [1981] did, or by using the correlation for the smallest nonzero lag to obtain the standard first-order autoregressive (AR(1)) fit to the lagged correlations, which would be the optimal procedure if the time behavior were exactly AR(1). Our approach is less sensitive to whether the lagged correlations are precisely exponential in behavior, yet produces the characteristic time scale of the process. The time scales we obtain do not differ substantially from *Laughlin*'s [1981], in any case.

An example of the lagged correlation of $\overline{r_A}(t)$ for the largest GATE area ($L = 280$ km) is shown in Figure 5 for phases I and II. The correlation time for GATE I is estimated to be approximately 7.7 hours. The lagged correlation of the model is also shown and will be discussed later. Correlation times obtained from analyzing GATE I data for three sizes of area A are plotted in Figure 6, with error bars representing 95% confidence limits. The error bars were obtained assuming that $\overline{r_A}$ behaves like an AR(1) process with Gaussian statistics, and may therefore err on the small side. Note that the time scales range from a half hour to nearly 8 hours in GATE. The model results, also shown in Figure 6, will be discussed below.

In order to establish the time scale to associate with each coefficient $a(\mathbf{k}, t)$ in the model, we shall assume that the time scale is a power of $k = |\mathbf{k}|$,

$$\tau_{\mathbf{k}} = ck^{-b} \tag{18}$$

and adjust the parameters b and c until the model's τ_A agree with those in GATE. The parameter values that result are given in Table 1. Figure 5 shows the correlation behavior of the model for a 280 × 280 km^2 area, which agrees well for lags near $\tau_A = 7.7$ hours but indicates that the GATE data might be better described by higher order autoregressive processes. We have nevertheless not attempted to use a higher order AR process to improve the fit, since it is difficult to justify the effort, given the length of the GATE time

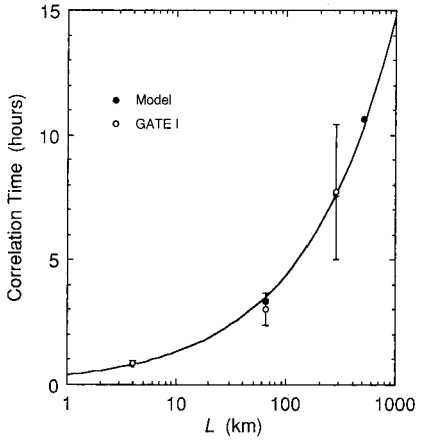

Fig. 6. Correlation times of area-averaged rain, based on lag when correlation has decreased to $1/e$, as function of area size L. Model values are based on a 300-day simulation. GATE values are from the 18 days of phase I. Error bars for GATE values show 95% confidence limits assuming a first-order autoregressive process with Gaussian statistics.

series, and the neglect of the slightly higher correlations for small lags only means that our estimate of E will err on the conservative (large) side.

Figure 6 shows the range of correlation times for different area sizes, and a power law fit

$$\tau_A = 0.394\, L^{0.525} \tag{19}$$

through the model data. The model is evidently capable of reproducing the range of time scales found in rainfall data. Note that, in effect, it also serves to extrapolate the GATE results to the larger area (L = 512 km) of interest to us. The model value of τ_A for this area was found to be 10.6 hours and the variance $\sigma_A^2 = 0.177$ mm^2/h^2.

5. Monte Carlo Method of Obtaining E

Once the statistical properties of the model are determined, a Monte Carlo estimate of the rms error (6) is in principle obtained by simulating many months of rainfall, and computing the rms difference between the satellite estimate (4) and the true mean (1). If we let $\hat{R}^{(\alpha)}$ and $R^{(\alpha)}$ be the estimated and true mean rain rate during month α, respectively, and define

$$\Delta R^{(\alpha)} = \hat{R}^{(\alpha)} - R^{(\alpha)} \tag{20}$$

to be the error for that month, a Monte Carlo estimate of E based on N simulated months would be

$$\hat{E}^2 = \frac{1}{N} \sum_{\alpha=1}^{N} (\Delta R^{(\alpha)})^2 \tag{21}$$

and the standard error of this estimate would be

$$\sigma(\hat{E}^2) = \frac{1}{N^{1/2}} \{\text{var}\,[(\Delta R^{(\alpha)})^2]\}^{1/2} \tag{22}$$

The Monte Carlo accuracy is proportional to $N^{-1/2}$. It is possible to increase the accuracy of the Monte Carlo calculation by estimating the rms error E for 6-day averages instead of for 30-day averages, based on the following argument.

In *Laughlin*'s [1981] derivation (reviewed by *Shin and North* [1988]), the sampling times t_i in (3) were assumed to start at $t = 0$, with $t_i = (i-1)\Delta t$, $i = 1, \cdots, M$, $T = M\Delta t$. If instead we assume that the sampling starts at $t = (1/2)\Delta t$, so that $t_i = (i - 1/2)\Delta t$, and repeat Laughlin's calculation, we obtain an expression for the error E of the form

$$E^2 = \sigma_A^2 \frac{\tau_A}{T}\left(L_1 + L_2 \frac{\tau_A}{T}\right) + O(e^{-T/\tau_A}) \tag{23}$$

with

$$L_1 = \frac{\Delta t}{\tau_A}\frac{1+r}{1-r} - 2 \tag{24a}$$

$$L_2 = -2\left(1 - \frac{\Delta t}{\tau_A}\frac{r^{1/2}}{1-r}\right)^2 \tag{24b}$$

$$r \equiv \exp(-\Delta t/\tau_A) \tag{24c}$$

If typical values for Δt in the range 12–24 hours and τ_A = 10.6 hours are used to evaluate L_2/L_1, the ratio is found to be well under 0.1. Equation (23) implies that for sampling typical of TRMM the mean square sampling error E^2 scales with averaging time T as

$$E^2 \sim 1/T \tag{25}$$

to an accuracy of a few percent or better for $T \geq 6$ days. We make use of this by dividing the sampling pattern of the satellite during a month into five 6-day periods with the division points occurring well away from satellite observation times. We then estimate the error E^2 for each 6-day period using Monte Carlo methods, average the errors together, and scale down by a factor of 5 as (25) dictates, and thereby obtain the error E^2 for 30-day means. By using this device, we are able to get 5 times as many samples from a given length simulation and so reduce the Monte Carlo error given in (22) by a factor of $5^{1/2}$, at the expense of a slightly more complicated analysis of the results.

Since the model generates four rain fields (the four quadrants of the 1024 × 1024 km^2 grid) with each time step, the error E^2 is calculated from the average errors found for each quadrant. The four quadrants are not completely independent, due to spatial correlation across the boundaries, and so the Monte Carlo error is not reduced by a simple factor of $4^{1/2}$ but by something smaller. The effective number of independent samples available from the four quadrants was estimated by comparing the variance among the four quadrant results in each 6-day sample with the variance in the results from any single quadrant. Uncertainty estimates in the Monte Carlo results presented in the next section are based on the product of the effective number of independent samples provided by the four quadrants and the number of 6-day samples entering into the average (20).

6. Monte Carlo Results

The model was tested to verify that its output statistics agree with those specified in Table 1. To test the Monte Carlo method, a calculation of the sampling error for T = 30 days, following the procedure outlined in the previous section (i.e., based on 6-day samples), was carried out

assuming observations every 12 hours of the entire 512 × 512 km^2 area. The Monte Carlo estimate from a 300-day simulation agreed with Laughlin's analytical result to within the uncertainty (22).

The sampling error associated with TRMM-like satellite observational patterns was first obtained for 30° inclination satellite orbits at two altitudes, 300 and 450 km. The error E was evaluated for rainfall averages over 512 × 512 km^2 boxes centered at two latitudes, 5°N and 25°N, assuming GATE-like statistics as specified in Table 1 at both locations. The observational patterns of the satellite were obtained for a 30-day orbit, calculated as in section 2, and broken up into 6-day periods with the break points well away from the times when the clusters of satellite observations (illustrated in Figure 1) occur. For the 25° latitude box, the sampling patterns (both altitudes) in each period were similar enough that the error E^2 was computed from a 300-day Monte Carlo run sampled according to a single representative 6-day period. For the 5° latitude case, the error E^2 was computed from the average of the errors found for each of the five periods in the month, using 60-day Monte Carlo simulations for each. The average error E^2 for a 6-day period was then scaled down by a factor of 5 to obtain an estimate of the 30-day sampling error, as described in the previous section.

Results are plotted in Figure 7 as a function of altitude, with a power law interpolation between the estimates at the two altitudes. The shaded area indicates $\pm\sigma$ limits from (22), converting the uncertainty in $\hat{E}^2$ to the uncertainty in $\hat{E}$ using the relation

$$\sigma(\hat{E}) = \sigma(\hat{E}^2)/2\hat{E} \tag{26}$$

valid for small normally distributed deviations about the true mean (i.e., $\sigma(\hat{E}) \ll E$). The error $\hat{E}$ is expressed as a percentage of the mean $\langle r\rangle$ = 0.445 mm/h.

The errors decrease with altitude because the areal coverage of the satellite observations increases with height. The error decreases more quickly for the 5°N box because at 300 km the satellite observes on average scarcely half the box every 12 hours, whereas at 450 km it is observing more nearly the whole box every 12 hours; for the box at 25°N the extra information obtained from the higher orbit is not as valuable, since the extra observations all occur within a few hours of observations already available from the lower orbit (cf. Figure 1), and there is still a large observational time gap each day.

A similar Monte Carlo calculation was carried out for a 35° inclination orbit at 350-km altitude, which may be nearer the best orbit for TRMM [*Simpson et al.*, 1988], for boxes at the same two latitudes. For this orbit the sampling error found was

$$E(5°\text{N})/\langle r\rangle = (8.3 \pm 0.7)\% \tag{27a}$$

$$E(25°\text{N})/\langle r\rangle = (7.2 \pm 0.5)\% \tag{27b}$$

(Uncertainty is $\pm\sigma$.) The error at 5°N is not appreciably changed by the increase in the orbital inclination. The error at 25°N is slightly reduced, presumably because the satellite samples are spread out over a greater portion of the day.

A crude idea of the sensitivity of the sampling error estimates to the various parameters can be obtained from the Laughlin-type estimate, (23)–(24). In the limit $\Delta t \gg \tau_A$, $L_1 \approx \Delta t/\tau_A$ and

$$E^2 \sim \sigma_A^2 \Delta t/T \tag{28}$$

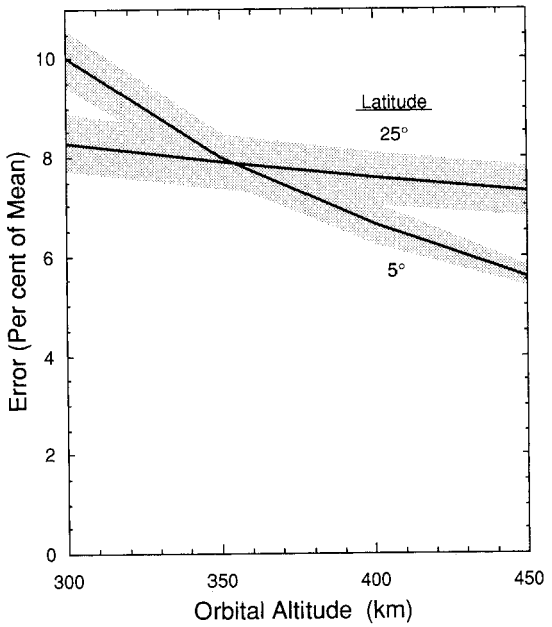

Fig. 7. Estimated rms sampling error for monthly averaged rainfall over a 512 × 512 km^2 area observed by a satellite in a 30° inclination orbit, as a fraction of the mean rain rate $\langle r\rangle$ = 0.445 mm/h, for areas centered at latitudes 5°N and 25°N. The shaded areas denote $\pm\sigma$ confidence limits determined by the 300-day Monte Carlo experiments.

The variance of area-averaged rain rate can be approximated, from (16), as

$$\sigma_A^2 \sim \text{var}\,(r) A^{-1} \int_0^L s c_r(s)\, ds \tag{29}$$

where $A = L^2$ and $c_r(s)$ is the spatial correlation of rain rate at points separated by distance s. The variance of rain rate in 4-km grid boxes, var (r), is approximately $p\sigma^2(r > 0)$, where $\sigma^2(r > 0)$ is the variance of rain rate over rainy areas only, and p is the average fraction of the area where it is raining at any one instant. Combining these approximations, we see that sampling error, expressed as a fraction of the mean rain rate $\bar{r} = p\bar{r}(r > 0)$, is

$$\frac{E}{\bar{r}} \sim \frac{1}{p^{1/2}} \frac{\sigma(r > 0)}{\bar{r}(r > 0)} \left(\frac{L_{\text{corr}}^2}{A}\right)^{1/2} \left(\frac{\Delta t}{T}\right)^{1/2} \tag{30}$$

where L_{corr} is the "correlation length"

$$\left[\int_0^L s c_r(s)\, ds\right]^{1/2}$$

which would be independent of L for large L if spatial correlations decrease fast enough. Thus the percent error grows as p or the averaging area A or averaging time T decreases. The sampling error is relatively insensitive to the correlation time τ_A, at least for $\Delta t \gg \tau_A$, but decreases with either Δt or τ_A more rapidly than (30) indicates for $\Delta t \leqslant \tau_A$. Note that the dependence of sampling error on how much of the area is viewed by the satellite (that is, the values of f_i in (2), which are determined by the satellite orbit and viewing angles) is not captured by the approximation (30).

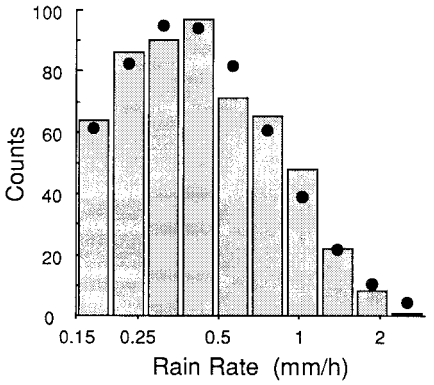

Fig. 8. Histogram of instantaneous rain rate averaged over 512 × 512 km^2 of the model. The samples are taken every 10 hours from a 300-day simulation, for a total of 720 samples. The bins are uniformly spaced in ln r, starting at ln $r = -1.91$ with spacing 0.3. The solid dots show the expected counts for a lognormal fit, with parameters $\langle \ln r \rangle = -1.016$ and $\sigma(\ln r) = 0.776$.

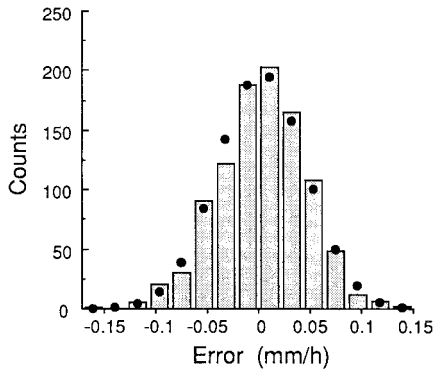

Fig. 9. Histogram of errors ΔR of satellite estimates of 30-day averaged rain rate (20) for a satellite in a 30° inclination orbit at 300 km, observing a 512-km square at 5°N. See text for details. Expected counts for each bin for a normally distributed variable are indicated by the dots. The parameters of the fit are $\langle \Delta R \rangle = 0.004$ mm/h and $\sigma(\Delta R)$ 0.043 mm/h.

7. Probability Distribution of Errors

The usefulness of the rms error estimate E depends somewhat on the probability distribution of the errors. If the errors are normally distributed, one expects the error for a given month's estimated rain rate to be smaller than $2E$, 95% of the time. Rainfall is notorious for its highly skewed distributions, however, and normality of the error distribution cannot be taken for granted. In fact, it seems that while rain rate is not normally distributed, the errors may be.

We show in Figure 8 the distribution of instantaneous rainfall averaged over a 512 × 512 km^2 of the model, from a 300-day simulation sampled every 10 hours in order to obtain relatively independent samples. Since only 5% of the total rain comes from area-averaged rain rates less than 0.15 mm/h, we show only the portion of the histogram for rain rates above 0.15 mm/h. The histogram bin sizes are logarithmic (note horizontal axis), so that if the rain rates were lognormally distributed, the histogram would appear Gaussian in shape. Since the samples are taken every 10 hours and the correlation time is 10.6 hours, the samples may be considered nearly independent.

A Gaussian fit to the histogram is shown by the dots on the figure; the agreement of the two as measured by a chi-square test is excellent. A lognormal distribution thus seems to describe area-averaged rain rate well, as least for rain rates that contribute significantly to rain volume. Although the model is forced to generate lognormally distributed rain on the scale of the grid squares, the spatial correlation in the model seems sufficiently strong to extend this behavior out to much larger scales. The central limit theorem might have suggested that the statistics of large-area averages would tend toward a normal distribution; and this would certainly have been the case had there been no spatial correlation. There may be a tendency for the largest rain rates to occur at slightly less than the frequency predicted by the lognormal distribution. Low rain rates, not shown in the figure, tend to occur more often than a lognormal distribution would predict. In any case, there is little doubt that instantaneous rain rates, even averaged over a 512- km box, are far from being normally distributed.

The error histogram for the difference between satellite-inferred monthly averaged rain rate and the true rain rate (20) is shown in Figure 9. These values are for a box at 5°N viewed by a satellite in a 30° inclination orbit at 300-km altitude. As was described in section 5, the simulations actually generated errors for 6-day averages and were combined to give 30-day errors. The histogram in Figure 9 is the result of a similar process; a month of satellite observations was divided into 5 periods, each 6 days long, as described in section 5. Given each 6-day period, with its corresponding satellite sampling pattern, rainfall was simulated by the model for 6 days at a time and observed according to the pattern for that period. This procedure produced a value for the 6-day sampling error defined as in (20). After many 6-day runs of the model, a table of errors was assembled for each 6-day portion of the month. Errors for 30-day averages were then created by taking five random selections from the table, one for each period, and averaging. The distribution of errors thus obtained is what is shown in Figure 9. This method of proceeding in effect introduces four artificial discontinuities in the rainfall during the course of a month, but it is unlikely that these substantially alter the distribution of errors, since rainfall in the model is not much correlated beyond 10 or 12 hours.

The errors obtained are consistent with a normal distribution, as shown by the fit (dots), and easily pass a chi-square test for goodness of fit.

8. Discussion and Conclusions

The size of the sampling error we estimate for a TRMM-like satellite is encouragingly small, less than 10%. If relatively unbiased rain rate retrieval schemes can be devised for the mission, even if accurate only to a factor of 2 per footprint (FOV), then sampling error will largely determine the accuracy of the monthly climatologies provided by the satellite. The sampling error may be reduced still further by incorporating information from other satellites.

The error estimate we obtain depends of course on our assumptions about the statistics of the rain being observed. These are all based on a few months of GATE statistics from one 400-km-diameter spot on the globe near the ITCZ. Rainfall statistics vary with location, and it will be important to quantify this variation as much as possible. Some inferences may be possible based on recent radar data obtained

from a number of locations and analyzed by *Atlas et al.* [this issue] and *Rosenfeld et al.* [this issue].

Even the estimates based on GATE data are subject to considerable uncertainty, as indicated by the sizes of the error bars in Figures 4 and 6 for quantities that largely govern the size of the sampling errors. Variations of this magnitude in the parameters might easily alter the size of E by as much as a factor of 2.

Our estimates of sampling error have not included the possibility of considerable aliasing of the results by diurnal and spatial variation of the statistics within an averaging box. The satellite offers the unique opportunity of exploring the diurnal cycle with its non-sun-synchronous orbit (cf. Figure 1), so that corrections for the diurnal cycle aliasing will be possible. *Bell* [1987*b*] has estimated that using TRMM data alone, and assuming GATE-like statistics, diurnal amplitudes of the order of 10% of the mean could be detected by averaging data over a 600 × 600 km^2 area and three seasons.

Clearly there is a great need for better knowledge of the variability of rainfall statistics in space and time and of how they depend on scale (from that of a rain gauge to thousands of kilometers). One of the happy outcomes of preparations for missions such as TRMM may be just this sort of knowledge.

Appendix: Estimate of Retrieval Error for Monthly Averages

Suppose that the satellite radiometers have a field of view (FOV) of the order of 10 km across [*Simpson et al.*, 1988] and that a retrieval scheme is developed which provides estimates of the average rain rate within the FOV,

$$\hat{r}_{\mathrm{FOV}} = (1 + \varepsilon) r_{\mathrm{FOV}} \tag{A1}$$

where r_{FOV} is the true rain rate averaged over the FOV, and we have assumed that the retrieval error can be represented by a positive definite multiplicative random variable $(1 + \varepsilon)$, with $\langle \varepsilon \rangle = 0$ for an unbiased retrieval scheme.

During 1 month of satellite observations of a 500 × 500 km^2 area, the satellite will return measurements of N FOVs from within the area, and the satellite estimate for the monthly mean will be

$$\hat{R}_{\mathrm{Retr}} = \frac{1}{N} \sum_{i=1}^{N} \hat{r}_{\mathrm{FOV},i} \tag{A2}$$

$$= \frac{1}{N} \sum_{i=1}^{N} r_{\mathrm{FOV},i} + \frac{1}{N} \sum_{i=1}^{N} \varepsilon_i r_{\mathrm{FOV},i} \tag{A3}$$

The first term on the right-hand side of (A3) is the "perfect instrument" estimate of the monthly mean, denoted $\hat{R}$ in (4). The second term is the retrieval error. The total error in retrieved monthly mean rain rate can thus be written

$$E_{\mathrm{Tot}}^2 = \left\langle \left[\hat{R} + \frac{1}{N} \sum_i \varepsilon_i r_{\mathrm{FOV},i} - R \right]^2 \right\rangle \tag{A4}$$

where R denotes the true monthly mean as in (1). If the retrieval errors are uncorrelated with the sampling error $\hat{R} - R$, this can be written

$$E_{\mathrm{Tot}}^2 = E^2 + E_{\mathrm{Retr}}^2 \tag{A5}$$

where E^2 is the sampling error (6), and with

$$E_{\mathrm{Retr}}^2 = \left\langle \left[\frac{1}{N} \sum_i \varepsilon_i r_{\mathrm{FOV},i} \right]^2 \right\rangle \tag{A6}$$

If we could assume that the retrieval error factor ε_i is unbiased and uncorrelated from one FOV to another, then

$$E_{\mathrm{Retr}}^2 = N^{-1} \langle \varepsilon_i^2 \rangle \langle r_{\mathrm{FOV}}^2 \rangle \tag{A7}$$

Let us suppose that retrievals from each FOV are only accurate to a factor of 2, or $\langle \varepsilon_i^2 \rangle \approx 1$. For a 10-km diameter FOV, $\langle r_{\mathrm{FOV}}^2 \rangle \approx 5$ mm^2/h^2 if we use the GATE statistics in Figure 4. Note that this estimate is an average over both rainy and nonrainy FOVs. One can carry out the error analysis treating separately the rainy and nonrainy FOVs, but the results are the same.

Near the equator the satellite views a 500 × 500 km^2 area about twice per day, or 60 times during a month. Assuming that it scans about half the area on each pass, we would estimate $N = 0.5 \times 60 \times (500 \text{ km})^2/(10 \text{ km})^2$ for a 10-km FOV, or $N = 75{,}000$. We would thus estimate the size of the retrieval error for monthly means to be

$$E_{\mathrm{Retr}} \approx 0.008 \text{ mm/h} \tag{A8}$$

or about 2% of the mean GATE rain rate (0.4 mm/h).

Acknowledgments. We gratefully acknowledge many helpful discussions with D. A. Short and thank L. S. Chiu and A. McConnell for sharing unpublished results with us. We would also like to thank D. Atlas, who long ago posed some of these problems to us. Research by two of the authors (A.A. and R.L.M.) was done under contract at Goddard Space Flight Center, Greenbelt, Maryland.

References

Aitchison, J., and J. A. C. Brown, *The Lognormal Distribution*, Cambridge University Press, New York, 1963.

Atlas, D., D. Rosenfeld, and D. A. Short, The estimation of convective rainfall by area integrals, 1, The theoretical and empirical basis, *J. Geophys. Res.*, this issue.

Bell, T. L., A space-time stochastic model of rainfall for satellite remote-sensing studies, *J. Geophys. Res.*, *92*, 9631–9643, 1987*a*.

Bell, T. L., Statistical properties in rainfall measurements from space, paper presented at the American Statistical Association Meeting, San Francisco, Calif., 1987*b*.

Brooks, D. R., An introduction to orbit dynamics and its application to satellite-based Earth monitoring missions, *NASA Ref. Publ. 1009*, 84 pp., Natl. Tech. Inform. Serv., Springfield, Va., 1977.

Houze, R. A., and A. K. Betts, Convection in GATE, *Rev. Geophys.*, *19*, 541–576, 1981.

Houze, R. A., Jr., and C.-P. Cheng, Radar characteristics of tropical convection observed during GATE: Mean properties and trends over the summer season, *Mon. Weather Rev.*, *105*, 964–980, 1977.

Hudlow, M. D., and V. L. Patterson, *GATE Radar Rainfall Atlas*, NOAA special report, 158 pp., U.S. Government Printing Office, Washington, D. C., 1979.

Kedem, B., L. S. Chiu, and G. R. North, Estimation of mean rain rate: Application to satellite observations, *J. Geophys. Res.*, *95*, 1965–1972, 1990.

Laughlin, C. R., On the effect of temporal sampling on the observation of mean rainfall, Precipitation measurements from space, workshop report, Goddard Space Flight Cent., Greenbelt, Md., 1981.

Leith, C. E., The standard error of time-average estimates of climatic means, *J. Appl. Meteorol.*, *12*, 1066–1069, 1973.

Rosenfeld, D., D. Atlas, and D. A. Short, The estimation of convective rainfall by area integrals, 2, The height area rainfall threshold (HART) method, *J. Geophys. Res.*, this issue.

Shin, K.-S., and G. R. North, Sampling error study for rainfall estimate by satellite using a stochastic model, *J. Appl. Meteorol.*, *28*, 1218–1231, 1988.

Simpson, J., R. F. Adler, and G. R. North, A proposed Tropical Rainfall Measuring Mission (TRMM) satellite, *Bull. Am. Meteorol. Soc.*, *69*, 278–295, 1988.

Wilheit, T., The electrically scanning microwave radiometer (ESMR) experiment, The Nimbus 5 user's guide, *Rep. 1972-735-963/259*, pp. 59–105, U.S. Govt. Printing Office, Washington, D. C., 1972.

A. Abdullah and R. L. Martin, Applied Research Corporation, Landover, MD 20785.

T. L. Bell, Laboratory for Atmospheres, Code 613, Goddard Space Flight Center, Greenbelt, MD 20771.

G. R. North, College of Geosciences, Texas A&M University, College Station, TX 77843.

(Received November 14, 1988;
revised March 22, 1989;
accepted April 19, 1989.)